ISSN 1063-7826, Semiconductors, 2018, Vol. 52, No. 2, pp. 215–220. © Pleiades Publishing, Ltd., 2018.
Original Russian Text © A.V. Stanchik, V.F. Gremenok, S.A. Bashkirov, M.S. Tivanov, R.L. Jušķénas, G.F. Novikov, R. Giraitis, A.M. Saad, 2018, published in Fizika i Tekhnika Poluprovodnikov, 2018, Vol. 52, No. 2, pp. 227–232.

MICROCRYSTALLINE, NANOCRYSTALLINE, POROUS, AND COMPOSITE SEMICONDUCTORS

Microstructure and Raman Scattering of $Cu_2ZnSnSe_4$ Thin Films Deposited onto Flexible Metal Substrates

A. V. Stanchik[a]*, V. F. Gremenok[a], S. A. Bashkirov[a], M. S. Tivanov[b], R. L. Jušķénas[c], G. F. Novikov[d], R. Giraitis[c], and A. M. Saad[e]

[a] *Scientific and Practical Materials Research Center, National Academy of Sciences of Belarus, Minsk, 220072 Belarus*
[b] *Belarusian State University, Minsk, 220030 Belarus*
[c] *State Research Institute "Center for Physical Sciences and Technology", Vilnius, 10222 Lithuania*
[d] *Institute of Problems of Chemical Physics, Russian Academy of Sciences, Chernogolovka, Moscow region, 142432 Russia*
[e] *Al-Balqa Applied University, Amman, 11953 Jordan*
**e-mail: alena.stanchik@bk.ru*

Submitted March 22, 2017; accepted for publication March 28, 2017

Abstract—$Cu_2ZnSnSe_4$ thin films are produced by selenizing electrochemically layer-by-layer deposited and preliminarily annealed Cu–Zn–Sn precursors. For flexible metal substrates, Mo and Ta foils are used. The morphology, elemental and phase compositions, and crystal structure of $Cu_2ZnSnSe_4$ films are studied by scanning electron microscopy, X-ray spectral microanalysis, X-ray phase analysis, and Raman spectroscopy.

DOI: 10.1134/S1063782618020197

1. INTRODUCTION

The quaternary compound $Cu_2ZnSnSe_4$ (CZTSe) is a promising direct-gap semiconductor material for use as light-absorbing layers in thin-film solar cells [1–3]. The CZTSe material exhibits a band gap of 1 eV, a high absorption coefficient for visible radiation ($>10^4$ cm^{-1}), *p*-type conductivity, and a maximum attainable efficiency of light-to-electricity conversion of 32.2% [4–6]. The traditional $CuIn_{1-x}Ga_xSe_2$ (CIGS) and CdTe materials contain expensive In, Ga, Te, and toxic Cd components [7, 8]. In contrast, the CZTSe material consists of abundant and nontoxic components, which makes it possible to reduce the recoupment period and to solve the problem of the recycling of used solar cells based on these components [4].

The idea of producing thin-film solar cells on flexible metal substrates has attracted more and more attention in recent years [9–11]. The advantages of light, flexible, and reliable (unbreakable) solar modules are obvious, especially for such fields of application as satellites, aviation, automotive equipment, and textile goods [10–13]. The possibility of using the roll-to-roll technology is as a rule the main argument in organizing the profit-making production of solar cells. If the technology is used in combination with nonvacuum methods of the deposition of CZTSe films (if possible), the production costs can be additionally reduced. However, at present, CZTSe thin films are most often synthesized by vacuum methods that call for complex and expensive equipment [4]. Compared to vacuum methods, the technique of the electrochemical deposition of precursors with their subsequent selenizing seems to be more attractive. This technique is distinguished by a low prime cost, simplicity of use, operation with nontoxic solvents and reagents, and possible mass manufacturing.

The purpose of this study is to analyze the influence of the substrate type (molybdenum or tantalum foils) on the microstructure of CZTSe thin films, including their morphology, elemental and phase compositions, and crystal structure. To refine the phase composition of CZTSe films, we here use Raman spectroscopy traditionally used for studies and the characterization of nanostructured materials without destruction or changes in their structure [14].

2. EXPERIMENTAL

The CZTSe thin films to be studied were produced by selenizing Cu–Zn–Sn (CZT) precursors electrochemically layer-by-layer deposited in the galvanostatic mode of operation in a two-electrode cell. The CZT precursors were deposited in layers in the sequence of Cu/Sn/Cu/Zn layers. For the anodes for deposition of the corresponding metal layers, we used industrial anodic copper, high-purity (99.999%) tin, and zinc wafers. The electrolytic solutions were prepared on the basis of solutions of the corresponding metal sulfates. Preliminary annealing of the deposited CZT precursors was conducted in 95% Ar + 5% H_2

Table 1. Elemental composition of CZTSe thin films on Mo and Ta substrates

Substrate	Elemental composition, at %				Ratio between elements	
	Cu	Zn	Sn	Se	Cu/(Zn+Sn)	Zn/Sn
Mo foil	25.07	15.39	10.14	49.40	0.98	1.51
Ta foil	22.09	18.53	10.83	48.54	0.75	1.71

atmosphere at a temperature of 350°C for 30 min, after which the precursors were cooled to room temperature. The annealed CZT precursors were selenized in a quartz container (with a volume of 12.5 cm^3) with 5 mg of powdery Se at an Ar gas pressure of 1 bar and a temperature of 580°C for 30 min.

The elemental composition of the films was determined by X-ray spectral (XRS) microanalysis, using a CAMECA SX-100 setup. The surface morphology of the CZTSe films was studied by scanning electron microscopy (SEM), using a Helios Nanolab (FEI company) electron microscope. The phase composition of the materials was studied using a Rigaku Ultima IV diffractometer operating with CuK_α radiation (at the wavelength $\lambda = 1.5406$ Å). Analysis of the phase composition was performed with the use of the database of the Joint Committee on the Powder Diffraction Standard (JCPDS) and the Crystallography Open Database (COD). The Raman spectra were recorded at room temperature, with a spectral resolution of no worse than 3 cm^{-1}. For Raman measurements, we used a Nanofinder HE (LOTIS TII) confocal Raman spectrometer. The Raman spectra were excited with a continuous solid laser emitting at a wavelength of 532 nm with an optical power of 0.2, 0.6, 1.6, and 2.0 mW. The diameter of the laser beam at the sample surface was ~0.6–0.7 μm.

3. RESULTS AND DISCUSSION

From the results given in Table 1, it follows that the composition of CZTSe films on Mo and Ta substrates slightly deviates from the stoichiometric relation (2 : 1 : 1 : 4). The atomic relations calculated for the CZTSe films on both of the substrates suggest that the composition is depleted of Cu and enriched with Zn, which corresponds to the criterion of high-efficiency thin-film solar cells based on CZTSe [4]. However, the value of the Zn/Sn ratio is larger than the value 1.2 indicated in [4], whereas the values of Cu/(Zn + Sn) for the film on Mo and Ta substrates are, correspondingly, somewhat smaller and larger than the optimal value 0.8 reported in [4].

It is known that the kesterite/stannite structure does not allow large deviations from the stoichiometric composition, which causes the formation of additional phases in the material [15, 16]. From the SEM images of CZTSe films (Fig. 1), it can be seen that different morphologies are formed depending on the elemental composition [17–19]. It is found that, at the surface of the CZTSe film on Mo substrate, small-sized and solitary large-sized crystallites are formed (Fig. 1a). In contrast, at the surface of the CZTSe film on Ta substrate, we observe a porous crystalline surface with large-sized crystallites (Fig. 1b). The bright regions observed at the surface of the CZTSe films are enriched with Zn and apparently correspond to the ZnSe phase [16]. The inference about the formation of the ZnSe phase at the surface of the films is consistent with the model suggested in [18] for the growth of CZTSe films enriched with Zn. According to this model, CZTSe crystals grow large and form a compact layer, leaving an excess of zinc at the surface. This effect results in the formation of the supplementary ZnSe phase.

In the SEM images of the cross sections of CZTSe films (Fig. 1), we can see $MoSe_2/TaSe_2$ layers at the interface between the Mo/Ta substrate and the CZTSe layer. The formation of $MoSe_2/TaSe_2$ layers apparently is a consequence of the high Se vapor pressure in the chamber during annealing of the film. This high pressure is favorable for the diffusion of Se through the layer of CZT precursors and for the reaction of Se with the substrate material [19].

The X-ray diffraction (XRD) patterns for CZTSe films (Fig. 2a, 2b) on both of the substrates exhibit high-intensity peaks characteristic of the tetragonal $Cu_2ZnSnSe_4$ phase (JCPDS 00-52-0868). Despite the fact that the peaks at $2\theta = 28.36°/28.42°$, 35.34°/35.44°, 38.70°/38.58°, and 42.86°/42.90° corresponding to the (103), (202), (114), and (213) planes of the $Cu_2ZnSnSe_4$ phase are lacking in the JCPDS 00-52-0868 database, these peaks are observed and confirmed in [20–23]. In the XRD patterns, there are also reflections from the Mo/Ta substrates and from the $MoSe_2$ (JCPDS 01-077-1715)/$TaSe_2$ (JCPDS 00-024-1257) phases formed upon selenizing the CZT precursors (Fig. 1a, 1b). The compositions of CZTSe films on both of the substrates can involve also the ZnSe phase (JCPDS 00-037-1463), whose principal reflections coincide with or are very close to the peaks of the $Cu_2ZnSnSe_4$ phase at $2\theta = 27.14°/27.22°$, 45.16°/45.06°, 53.46°/53.43°, and 65.74°/65.68°. In addition, in the XRD pattern of CZTSe film on Ta foil, there are low-intensity reflections of the CuSe phase (JCPDS 00-034-0171).

The lattice parameters calculated from the data of XRD analysis of CZTSe films (Table 2) are larger than

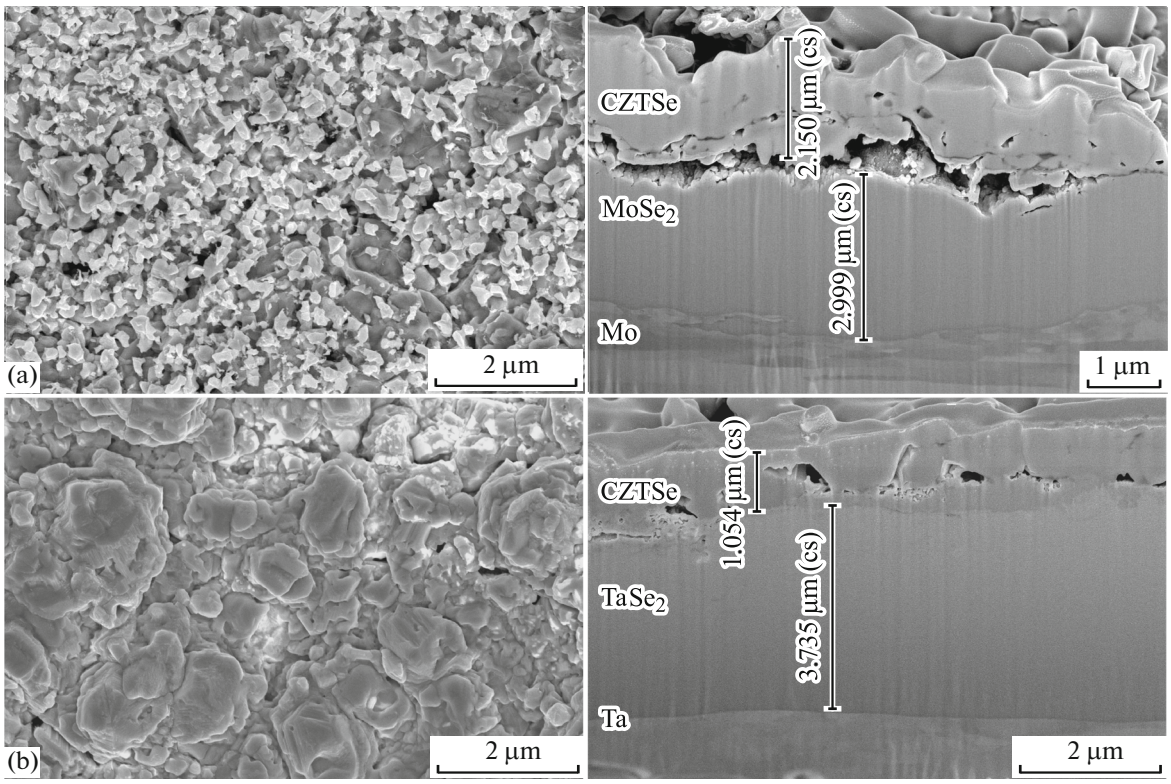

Fig. 1. SEM images of the surface and cross section of CZTSe films on (a) Mo and (b) Ta substrates.

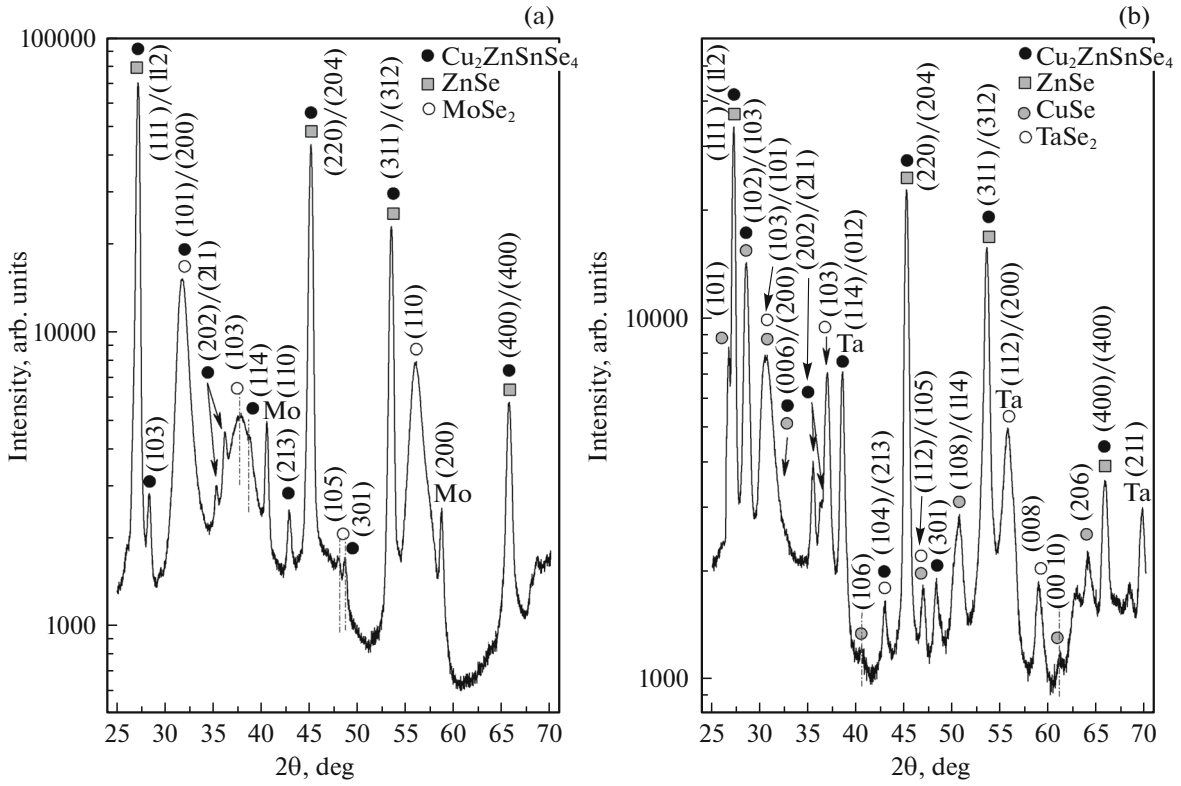

Fig. 2. XRD patterns of CZTSe films on (a) Mo and (b) Ta substrates.

Table 2. The lattice parameters of CZTSe thin films on Mo and Ta substrates

Substrate	a, Å	c, Å	η
Mo foil	5.707 ± 0.004	11.394 ± 0.002	0.998
Ta foil	5.705 ± 0.002	11.370 ± 0.008	0.996

the corresponding parameters reported in other studies [24, 25], which is in agreement with the data of [23].

From the results of XRD analysis, it is impossible to reliably determine which of the two structures, kesterite or stannite, has been formed. In [25], the XRD analysis of the $Cu_2ZnSnSe_4$ single crystal showed that the stannite structure exhibits the following lattice parameters: a = 5.6882 Å, c = 11.3378 Å, and η = 1.0034. According to [26], the CZTSe compound can crystallize with the formation of both of the above-mentioned structures, but in the case of kesterite, the lattice parameter a is bound to be somewhat larger and the trigonal distortion η somewhat smaller compared to the corresponding parameters of the stannite structure. In addition, one more structure that can be formed by the CZTSe alloy is partially disordered kesterite [27]. The disorder of the Cu + Zn layer induces a volumetric expansion of up to 0.3% [27]. Taking into consideration the above-listed structural features of kesterite and stannite and the results of this study, we can conclude that the electrochemically deposited CZT precursors are crystallized with the formation of the kesterite or partially disordered kesterite structure.

Figure 3 shows the typical Raman spectra of CZTSe films produced on Mo and Ta substrates. The spectra observed for CZTSe films on both of the substrates are very similar. The Raman bands observed at about 67, 80/81, 172, 196, 235/233, 243, and 386 cm^{-1} (Figs. 3a, 3b) are typical of the kesterite-structured CZTSe compound [23, 28–36].

As shown in [31], the broad Raman band at about 172 cm^{-1} can be formed by two Raman-active mode of A symmetry in CZTSe kesterite. In this study, the ~172 cm^{-1} Raman band is formed by a single mode. The full width at half-maximum (FWHM) of this band is ~9.94 cm^{-1}. The 191/196 cm^{-1} principal peak in the Raman spectra of CZTSe films on both of the substrates is asymmetrically broadened [23, 31, 32]. Such broadening of the 191/196 cm^{-1} peak can be attributed to the phonon confinement effect, as shown

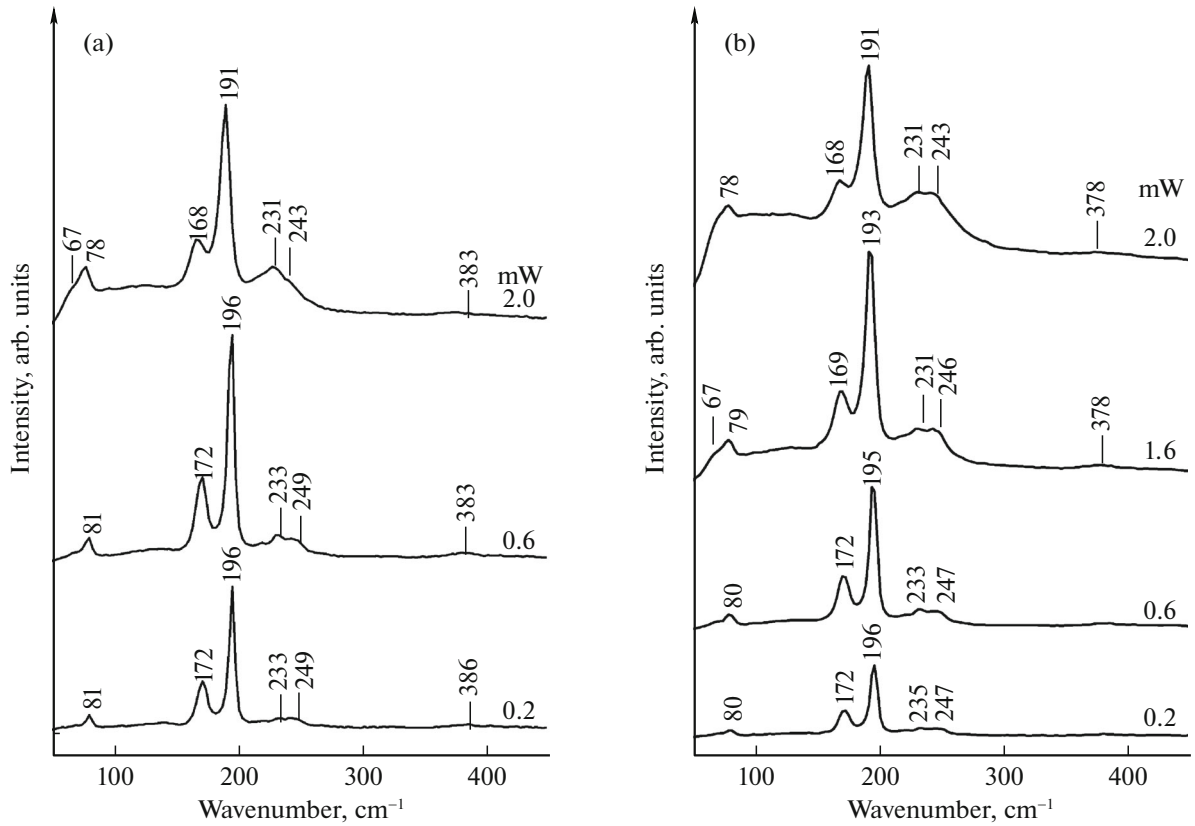

Fig. 3. Raman spectra of CZTSe films on (a) Mo and (b) Ta substrates in the range of wave numbers from 50 to 450 cm^{-1} at different laser excitation powers (532 nm).

in [31]. The low-intensity 247/249 cm^{-1} bands correspond to the energy of longitudinal optical (LO) phonons in the cubic ZnSe modification [23]. The experimentally observed shift of this band to lower photon energies with respect to the energies known for bulk ZnSe (252–256 cm^{-1}) corresponds to ZnSe nanoparticles [23]. In the Raman spectra obtained here for CZTSe films on Mo and Ta substrates, no characteristic lines of the $MoSe_2$ and $TaSe_2$ phases [18, 23, 30, 32–34] are observed. This is indicative of the lack of these phases in CZTSe layer and is consistent with the transverse SEM images (Fig. 1) which suggest the formation of the $MoSe_2/TaSe_2$ phases only at the interface between the CZTSe film and Mo/Ta substrate. The 91 and 260–270 cm^{-1} bands characteristic of the CuSe phase detected by XRD analysis of the composition of CZTSe films on the Ta substrate are not observed in the Raman spectra [23, 32, 35]. One of the possible causes of such a result is the very low efficiency of Raman scattering in this phase [32, 33].

The wave number of the most intense characteristic band of *A* symmetry for CZTSe decreases from 196 to 191 cm^{-1}, as the laser power is increased from 0.2 to 2.0 mW (Figs. 3a, 3b). In addition, the FWHM of this band increases from 5.6 to 8.3 cm^{-1} and from 6.9 to 9.6 cm^{-1} for the films on the Mo and Ta substrates, respectively. It should be noted that the frequency of the band with a lower intensity, 172 cm^{-1}, also becomes lower at a higher excitation level. The decrease in the phonon frequency of the *A* mode in the kesterite structure with increasing temperature (laser power) can be explained in the context of the perturbation model, in which the frequency shifts due to the combined effect of such factors as thermal expansion and anharmonic phonon–phonon interaction [36].

4. CONCLUSIONS

Thin CZTSe films are produced by selenizing CZT precursors electrochemically deposited in layers onto flexible Mo and Ta metal foils. It is found that the morphology and phase composition of the CZTSe films depend on the relation between the constituent elements in the film. X-ray phase analysis of the CZTSe films on Mo and Ta substrates shows the presence of $Cu_2ZnSnSe_4$ basic phase and $MoSe_2/TaSe_2$ and ZnSe phases. The CZTSe films on the Ta substrate show reflections of the CuSe phase as well. From the data of XRD analysis, the lattice parameters of CZTSe are determined. These are $a = 5.707 \pm 0.004$ Å, $c = 11.394 \pm 0.002$ Å, and $\eta = c(2a)^{-1} = 0.998$ for films on the Mo substrate and $a = 5.705 \pm 0.002$ Å, $c = 11.370 \pm 0.008$ Å, and $\eta = c(2a)^{-1} = 0.996$ for films on the Ta substrate. The Raman data for CZTSe films on the Mo and Ta substrates supports the inference about the formation of $Cu_2ZnSnSe_4$ and ZnSe phases. Analysis of the XRD and Raman data obtained in the study shows that the CZTSe films on both of the substrates are kesterite-structured. The formation of the $MoSe_2$ and $TaSe_2$ phases at the interface between the CZTSe layer and the substrate is confirmed by XRD analysis, Raman data, and SEM images of the cross section of CZTSe films.

The results of this study can be used for further development of the technology for production of CZTSe thin films to be used in a new generation of thin-film elements.

ACKNOWLEDGMENTS

The study was supported by the State Program of Scientific Research "Physical Material Science, New Materials and Technologies", the Belarusian Republican Foundation for Fundamental Research, and the Russian Foundation for Basic Research, project no. 16-08-01234.

REFERENCES

1. M. A. Green, K. Emery, Y. Hishikawa, W. Warta, and E. D. Dunlop, Prog. Photovolt.: Res. Appl. **24**, 905 (2016).
2. S. A. Bashkirov, R. Kondrotas, V. F. Gremenok, R. L. Yushkenas, and I. I. Tyukhov, International Scientific Journal for Alternative Energy and Ecology **15–18**, 31 (2016).
3. V. V. Rakitin and G. F. Novikov, Russ. Chem. Rev. **86**, 99 (2017).
4. M. P. Paranthaman, W. Wong-Ng, and R. N. Bhattacharya, *Semiconductor Materials for Solar Photovoltaic Cells* (Springer International, Switzerland, 2016), Vol. 218, p. 25.
5. K. Ito and T. Nakazawa, Jpn. J. Appl. Phys. **27**, 2094 (1988).
6. W. Shockley and H. J. Queisser, J. App. Phys. **32**, 510 (1961).
7. M. A. Green, Prog. Photovolt.: Res. Appl. **17**, 347 (2009).
8. P. D. Moskowitz and V. M. Fthenakis, Solar Cells **29**, 63 (1990).
9. K. Otte, L. Makhova, A. Braun, and I. Konovalov, Thin Solid Films **511–512**, 613 (2006).
10. F. Kessler, D. Herrmann, and M. Powalla, Thin Solid Films **480–481**, 491 (2005).
11. M. Pagliaro, G. Palmisano, and R. Ciriminna, *Flexible Solar Cells* (Wiley-VCH, Italy, 2008).
12. A. Jasenek and U. Rau, Appl. Phys. Lett. **90**, 650 (2001).
13. A. V. Stanchik, S. M. Baraishuk, S. A. Bashkirov, V. F. Gremenok, M. S. Tivanov, M. B. Dergacheva, and K. A. Urazov, Izv. NAN Belarusi, Ser. Fiz.-Mat. Nauk, No. 4, 67 (2016).
14. A. V. Baranov, K. V. Bogdanov, E. V. Ushakova, S. A. Cherevkov, A. V. Fedorov, and S. Tscharntke, Opt. Spectrosc. **109**, 268 (2010).

15. I. D. Olekseyuk, I. V. Dudchak, and L. V. Piskach, J. Alloys Compd. **368**, 135 (2004).
16. J. J. Scragg, P. J. Dale, and L. M. Peter, Thin Solid Films **517**, 2481 (2009).
17. H. Xie, M. Dimitrievska, X. Fontane, Y. Sanchez, S. Lopez, V. Izquierdo, V. Bermudez, A. Perez, and E. Saucedo, Solar Energy Mater. Solar Cells **140**, 289 (2015).
18. R. Kondrotas, R. Juskenas, A. Naujokaitis, A. Selskis, R. Giraitis, Z. Mockus, S. Kanapeckaite, G. Niaura, H. Xie, Y. Sanchez, and E. Saucedo, Solar Energy Mater. Solar Cells **132**, 21 (2015).
19. J. J. Scragg, PhD Dissertation (Univ. of Bath, UK, 2010).
20. H. Matsushita, T. Maeda, A. Katsui, and T. Takizawa, J. Cryst. Growth **208**, 416 (2000).
21. G. Zoppi, I. Forbes, R. W. Miles, P. J. Dale, J. J. Scragg, and L. M. Peter, Prog. Photovolt.: Res. Appl. **17**, 315 (2009).
22. J. Mao, S. Zhang, X. Peng, J. Zhang, H. Zhang, L. Gu, and Y. Xiang, Vaccum (2015). doi 10.1016/j.vacuum.2015.01.015
23. R. Juskenas, S. Kanapeckaite, V. Karpaviciene, Z. Mockus, V. Pakstas, A. Selskiene, R. Giraitis, and G. Niaura, Solar Energy Mater. Solar Cells **101**, 277 (2012).
24. P. M. P. Salome, P. A. Fernandes, J. P. Leita, M. G. Sousa, J. P. Teixeira, and A. F. Cunha, J. Mater. Sci. **49**, 7425 (2014).
25. I. D. Olekseyuk, L. D. Gulay, I. V. Dydchak, L. V. Piskach, O. V. Parasyuk, and O. V. Marchuk, J. Alloys Compd. **340**, 141 (2002).
26. S. Chen, X. G. Gong, A. Walsh, and S.-H. Wei, Appl. Phys. Lett. **94**, 041903 (2009).
27. S. Schorr, Thin Solid Films **515**, 5985 (2007).
28. A. Khare, B. Himmetoglu, M. Johnson, D. J. Norris, M. Cococcioni, and E. S. Aydil, J. Appl. Phys. **111**, 083707 (2012).
29. R. Juskenas, G. Niaura, Z. Mockus, S. Kanapeckaite, R. Giraitis, R. Kondrotas, A. Naujokaitis, G. Stalnionis, V. Pakstas, and V. Karpaviciene, J. Alloys Compd. **655**, 281 (2016).
30. G. Niaura, R. Juskenas, V. F. Gremenok, A. V. Stanchik, S. A. Bashkirov, M. S. Tivanov, O. V. Korolik, A. M. Saad, W. Y. Kim, and S. H. Chai, in *Proceedings of the 7th International Scientific Conference on Actual Problems of Solid State Physics* (Minsk, Belarus, 2016), Vol. 1, p. 264.
31. R. Djemour, A. Redinger, M. Mousel, L. Gütay, X. Fontane, V. Izquierdo-Roca, A. Perez-Rodríguez, and S. Siebentritt, Opt. Express **21** (S4), A695 (2013).
32. A. Redinger, K. Hönes, X. Fontane, V. Izquierdo-Roca, E. Saucedo, N. Valle, A. Perez-Rodríguez, and S. Siebentritt, Appl. Phys. Lett. **98**, 101907 (2011).
33. V. Izquierdo-Roca, E. Saucedo, C. M. Ruiz, X. Fontané, L. Calvo-Barrio, J. A. Garcia, P.-P. Grand, J. S. Jaime-Ferrer, A. Pérez-Rodríguez, J. R. Morante, and V. Bermudez, Phys. Status Solidi A **206**, 1001 (2009).
34. Z. Yan, C. Jiang, T. R. Pope, C. F. Tsang, J. L. Stickney, P. Goli, J. Renteria, T. T. Salguero, and A. A. Balandin, J. Appl. Phys. **114**, 204301 (2013).
35. J. Tao, J. Liu, J. He, K. Zhang, J. Jiang, L. Sun, P. Yan, and J. Chu, R. Soc. Chem. Adv. **4**, 23977 (2014).
36. P. K. Sarswat, M. L. Free, and A. Tiwari, Phys. Status Solidi B **248**, 2170 (2011).

Translated by E. Smorgonskaya